crease in optical field strength. Specifically, for our experiment the product of the level shifts of the 3*S* and 4*D* states is proportional to the two-photon transition rate. Optically induced energy-level shifts might also find practical applications. The intensity dependence of the shifts provides an accurate method for measuring transition dipole moments. In addition, the level shifts form the basis for a kind of Stark spectroscopy. Although all the hyperfine states of the 3*S* ground state had essentially equal shifts, hyperfine states of the 4*D* level have different shifts and hence should split. This splitting was masked by the line-broadening mechanisms discussed earlier but would be observable in an experiment utilizing a sodium atomic beam. Stark splitting of the 3*S* ground state could also be observed if the mistuning of the 589-nm light from the 3*P* resonance were made smaller than the hyperfine splitting of the 3*P* state.

The authors are grateful to J. P. Gordon for his interest and encouragement. We also acknowledge the invaluable technical assistance of D. B. Pearson.

[1]J. E. Bjorkholm and P. F. Liao, Phys. Rev. Lett. 33, 128 (1974).

[2]L. S. Vasilenko, V. P. Chebotaev, and A. V. Shishaev, Pis'ma Zh. Eksp. Teor. Fiz. 12, 161 (1970) [JETP Lett. 12, 113 (1970)]. Also see the second footnote of Bjorkholm and Liao, Ref. 1.

[3]See A. M. Bonch-Bruevich and V. A. Khodovoi, Usp. Fiz. Nauk 93, 71 (1967) [Sov. Phys. Usp. 10, 637 (1968)], for a comprehensive review of ac Stark effect theory and experiments.

[4]W. Happer, *Progress in Quantum Electronics* (Pergamon Press, Oxford, 1971), Vol. 1, Pt. 2, p. 51.

[5]A. M. Bonch-Bruevich, N. N. Kostin, V. A. Khodovoi, and V. V. Khromov, Zh. Eksp. Teor. Fiz. 56, 144 (1969) [Sov. Phys. JETP 29, 82 (1969)]; B. Dubreuil, P. Ranson, and J. Chapelle, Phys. Lett. 42A, 323 (1972).

[6]Two-photon transitions can be induced by either the term $(e/mc)\vec{p}\cdot\vec{A}$ or the term $e^2\vec{A}^2/2mc^2$ of the interaction Hamiltonian, where $\vec{p}$ is the electron momentum operator and $\vec{A}$ is the vector potential of the electromagnetic field. In general, the $\vec{A}^2$ term is negligible compared to the other. Two-photon transitions induced by $(e/mc)\vec{p}\cdot\vec{A}$ involve virtual intermediate atomic states.

[7]J. E. Bjorkholm and P. F. Liao, to be published.

[8]J. K. Link, J. Opt. Soc. Amer. 56, 1195 (1966).

[9]It has been incorrectly states in the literature that the level shifts are always less than power broadening; see, e.g., B. Cagnac, G. Grynberg, and F. Biraben, J. Phys. (Paris) 34, 845 (1973). Level shifts can occur in the absence of saturation if $P_{gm}\mathcal{E}_2$ differs from $P_{me}\mathcal{E}_1$, where P_{gm} (P_{me}) is the dipole moment matrix elements between the intermediate state m and the ground state g (excited state, e). $\mathcal{E}_1,\mathcal{E}_2$ are the electric field strengths of the photon fluxes involved.

[10]See R. F. Miles and S. E. Harris, IEEE J. Quant. Electron. 9, 470 (1973) for an example of such a situation in nonlinear optics. Frequency shifts will also occur in other two-photon processes; e.g., see R. G. Brewer and E. L. Hahn [Phys. Rev. A 8, 464 (1973)] for a calculation of the shift in the coherent Raman beat experiment.

Steady-State Distributions of Interacting Discrete Vortices

D. L. Book, Shalom Fisher, and B. E. McDonald
Plasma Dynamics Branch, Plasma Physics Division, U. S. Naval Research Laboratory, Washington, D. C. 20375
(Received 25 September 1974)

The sinh-Poisson equation describing two-dimensional steady-state distributions of elements with a logarithmic interaction potential (charged filaments executing guiding-center motion; quantized vortex lines) is solved numerically. Multiple solutions are obtained for the case of negative temperatures. These have a simple thermodynamic interpretation which agrees with the results of numerical simulations. The results are related to numerical experiments and observations of vortex filaments in liquid He^4.

It has been shown that statistical systems with bounded phase space can have negative-temperature states.[1] One such system is an aggregation of charged filaments executing guiding-center motion[2] within a finite region having conducting boundaries; another, equivalent mathematically, is a collection of interacting quantized vortices enclosed by reflecting walls. Numerical[3-5] studies of such systems reveal that they sometimes evolve to steady states characterized by large-scale charge circulation (in the first case) or widely separated regions of oppositely directed

vorticity (in the second). These results are consistent with the conclusion, reached on general thermodynamic grounds,[6] that a negative-temperature system displays a tendency to fly apart. The phenomenon of small vortices clumping into larger ones is not observed when initial conditions corresponding to an ordinary positive temperature are chosen.

Several analytic studies[4,7,8] have been carried out in order to clarify the statistical properties of negative-temperature systems. In particular, Joyce and Montgomery[4,8] have used the combinatorial method of Boltzmann to derive an equation for the electrostatic potential φ corresponding to the most probable steady state (or equivalently, the stream function of the most probable vortex distribution). This equation may be written

$$\nabla^2\varphi = -(4\pi e/l) \times [n_+ \exp(-e\beta\varphi) - n_- \exp(e\beta\varphi)], \quad (1)$$

where φ is the scalar potential, e the charge, and e/l the charge per unit length of a filament, the $n_\pm$ are constants related to the total number N of filaments of either species by

$$n_\pm \int d^3r \exp(\mp \beta e\varphi) = N, \quad (2)$$

and the inverse temperature β is determined by specifying the energy E,

$$l\int d^3r[(\nabla\varphi)^2/8\pi] = E. \quad (3)$$

The derivation of Eq. (1) is valid only for $\beta < 0$.

This equation is the same as that obtained if one looks for *stationary* positive-temperature states of any system of electrostatically interacting oppositely charged particles (of arbitrary finite mass) using Boltzmann statistics, and hence represents an extension of the Debye-Hückel theory.[9] It also describes the magnetic equilibrium[10] of a relativistic beam consisting of equal-temperature ion and electron components with the same rest frame. Behavior resembling that seen in the simulations of Joyce and Montgomery[4] has in fact been observed by Lee and Lampe[11] in studying the filamentation of relativistic beams. In these examples the two components can in principle have different temperatures ($\beta_+ \neq \beta_-$). Some of our results apply as well in this case, but we will not discuss them explicitly.

Equation (1) is conveniently rewritten as

$$\nabla^2\psi + \lambda^2 \sinh\psi = 0, \quad (4)$$

which we take as our standard form. Here $\psi = -e\beta\varphi - \frac{1}{2}\ln(n_+/n_-)$ and $\lambda^2 = -8\pi\beta(n_+n_-)^{1/2}e^2/l$. Since $-\lambda^2 \propto \beta = (\kappa T)^{-1}$, where κ is Boltzmann's constant (see Ref. 4), $\lambda^2 > 0$ formally describes negative temperatures. As a boundary condition on ψ we assume $\psi = 0$ on the periphery of a rectangular box of dimension X by Y; where no values are explicitly stated $X = Y = 1$ will be understood. The additional requirement of equal total numbers of positive and negative charges ($n_+ = n_- = n_0$) implies $\int\int dx\,dy\psi = 0$ must hold within the box.

The form of Eq. (4), together with the boundary conditions as stated, suggests the possibility of bifurcated solutions.[12,13] The one-dimensional Cartesian version of Eq. (4),

$$(d^2\psi/dx^2) + \lambda^2 \sinh\psi = 0, \quad (4')$$

with $\psi(0) = \psi(1) = 0$, is analytically solvable.[14] Some solutions are displayed in Fig. 1. There are an infinite number of discrete modes for each value of λ, but the types of modes which are accessible depend upon λ. The "s" mode, for example, does not exist for $\lambda > \pi$. For $\lambda > 2\pi$, neither the "s" nor the "p" mode exists. The critical values of λ are calculable from the linearized version of Eq. (4') with the same boundary conditions as in-

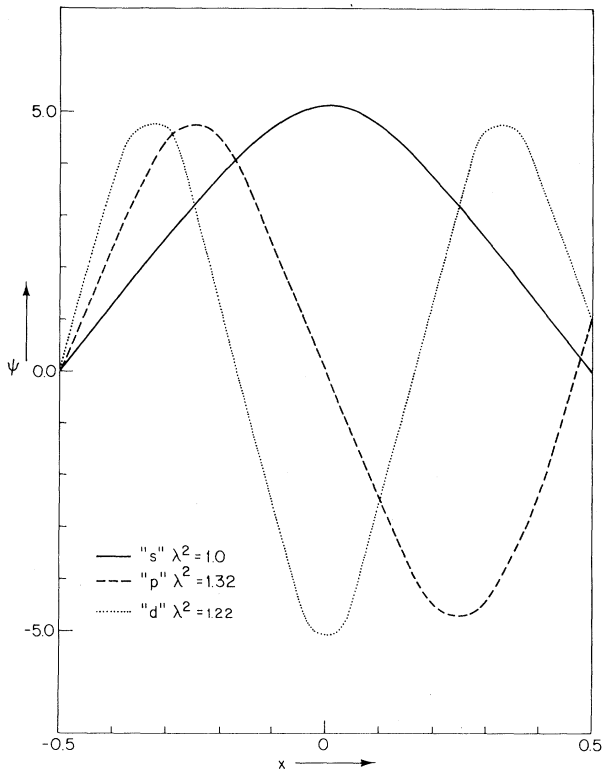

FIG. 1. Plots of ψ versus x showing s, p, and d modes for the one-dimensional case [Eq. (4')]. Three different values of λ^2 have been used so that solutions can be displayed using the same scale.

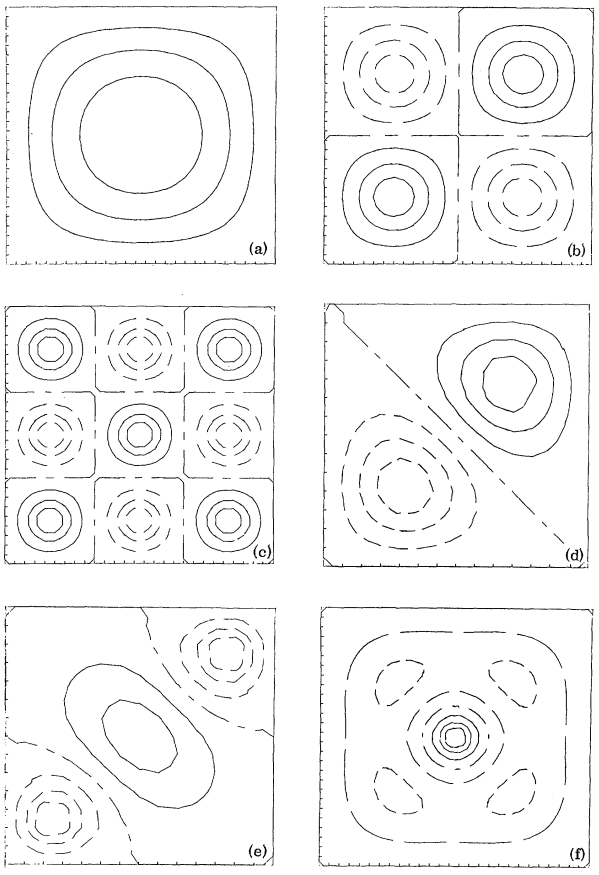

FIG. 2. Six solutions of Eq. (4) obtained with $\lambda^2 = 19.0$, designated (a)–(f) *s-s*, *p-p*, *d-d*, diagonal *s-p*, diagonal *s-d*, and diagonal *d-d*, respectively. Dashed lines are used to represent negative contour levels.

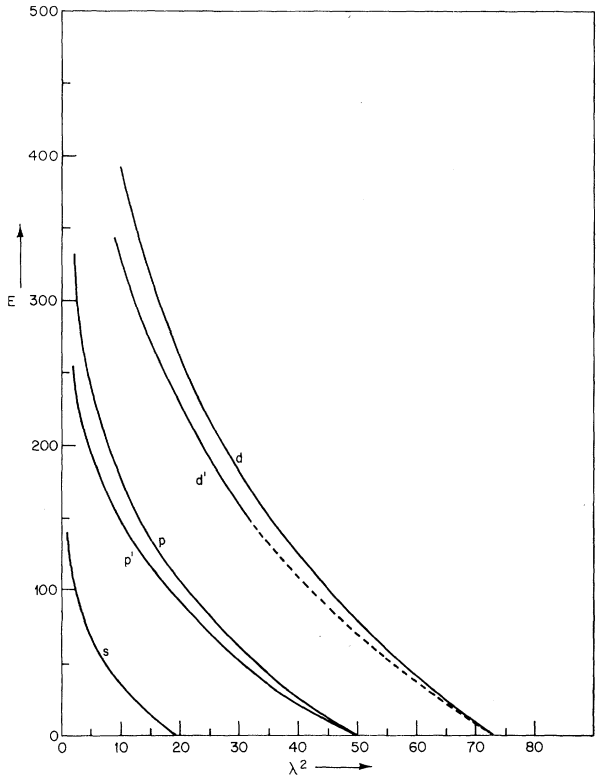

FIG. 3. E (arbitrary units) versus λ^2 for the modes *s-s*, *s-p*, diagonal *s-p*, *s-d*, and diagonal *s-d* (here labeled *s*, *p*, *p'*, *d*, and *d'*, respectively).

dicated. This is because the maximum amplitude, ψ_m, is a decreasing function of λ and vanishes as λ approaches a particular λ_0 for each mode. The qualitative behavior of amplitude as a decreasing function of λ for each mode carries over to the two-dimensional solutions as well.

The two-dimensional equation is solved by a numerical technique, the details of which are reported elsewhere.[15,16] It permits one to generate nontrivial solutions of Eq. (4) to any desired accuracy. It appears that an infinite number of such solutions exist, as in the one-dimensional case. These solutions can also be characterized by the type of internal symmetry and the number of nodes, or "quantum number," in each coordinate direction.

Figure 2 reproduces a series of contour plots of solutions obtained with $\lambda^2 = 19.0$. Solutions (a), (b), (c) are referred to as *s-s*–, *p-p*–, and *d-d*–wave solutions. (Evidently the *s-s*–wave solution does not satisfy the zero total-charge condition, but is included for completeness.) The higher-order solutions may be viewed as composed by patching together increasing numbers of *s*-wave images. Since $\psi = 0$ on each symmetry line, each subdivision of the box behaves like an independent "cell." One can construct mixed solutions (*s-p*, *s-d*, etc.) by an obvious extension of this process.

Figures 2(d)–2(f) show contours of solutions with diagonal symmetry. Just as with the family 2(a)–2(c), higher-order solutions can be found by patching together "diagonal *p*-wave" or "diagonal *d*-wave" solutions. The class of solutions which can be displayed in this fashion is limited by numerical considerations.[15] In principle, however, each such family contains a countably infinite number of members, and there may be other solutions as well.

The solutions shown in Fig. 2 each have a different energy E. By varying λ we can trace the distinct branches in a λ-E diagram (Fig. 3) until stymied by computational difficulties. Each branch extends down to the λ axis, where the in-

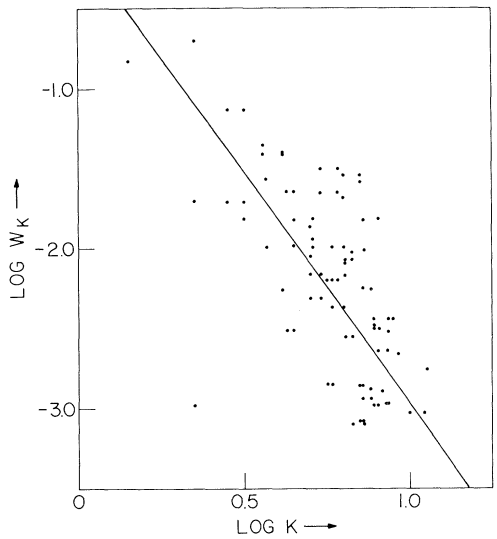

FIG. 4. Log-log plot of mode energy versus wave number for the diagonal s-p state with $\lambda^2 = 15.0$. The straight line through the points is obtained by a least-squares fit; its slope is -2.9, indicating a spectral density $\sim k^{-3}$.

tercept can be found from linear theory ($\sinh\psi \approx \psi$), and up to infinite E in analogy with the one-dimensional solution. The general character of these traces is in agreement with results found by analytic methods.[17]

What is the physical significance of this plethora of solutions of a mathematically well-posed problem? The argument leading to Eq. (1) specifies that entropy S be maximized by φ; evidently S has infinitely many *local* maxima as a functional of φ, to each of which corresponds a solution.[17] From the derivation of Eq. (1), it is easy to show that the entropy S of a solution ψ is given to within an additive constant by

$$S = \ln W = 2\beta E = -\frac{l}{4\pi e^2}\frac{\lambda^2}{n_0}E, \tag{5}$$

where W is the *a priori* probability of the configuration. Hence for n_0 and E specified, $W = W_0 \times \exp(-c\lambda^2)$, $c = \text{const} > 0$. The form (5) of the entropy is to be contrasted with that found for negative-temperature states of a two-level system, for example, of nuclear spins in an ionic lattice.[18] There $S = S_0 - \text{const}E^2$, and the energy varies only between finite limits $\pm E_{\max}$.

To compare our results with the simulations of Joyce and Montgomery,[4] we have redone the analysis for a $\frac{1}{2}\times 1$ box, equivalent to that used in the simulations. For equal numbers $n_+ = n_-$ the branch with maximum entropy is the s-p solution. For $\lambda^2 = 29.0$ (corresponding to $E = 98.85$), fair agreement is obtained with the result shown in Fig. 2 of Ref. 4. Since the simulation employed finite-sized particles and periodic boundary conditions, a temperature determined from a trace like those of Fig. 3 will not be reliable. The best way to assign a temperature to the result of the computer experiment would appear to be by fitting the energy spectrum of the theoretical solution to the observed spectrum.

We have also Fourier analyzed the solutions described above. Figure 4 shows the result for the diagonal s-p state shown in Fig. 2(d), with $\lambda^2 = 15.0$. Mode energy is plotted against k, the magnitude of the wave vector, for $0 < k_x < 2\pi$, $0 < k_y \leq \pi$. As can be seen, the points fall approximately in a straight line. A least-squares fit yields a slope of -2.9, in good agreement with the k^{-3} spectrum predicted by continuum theory for enstrophy cascade.[19]

In conclusion, we wish to call attention to the fact that the vortex filaments recently observed[20] in liquid He can be in negative-temperature states. For the present theory to apply, only the lowest quantum levels (circulation $= \pm h/m_{\mathrm{He}}$) must be excited, in equal numbers, and the interaction energy must be positive. Such a system could then be expected to evolve to a state with just two regions of vorticity, one of either sign. In fact, the detection of such a state would be convincing evidence that the aggregate of filaments possessed a negative temperature.

We wish to express our gratitude to Dr. D. Montgomery and Dr. L. Baker for several useful discussions.

[1]L. Onsager, Nuovo Cimento, Suppl. 6, 279 (1949).
[2]D. Montgomery, Phys. Lett. 39A, 7 (1972).
[3]G. S. Deem and N. J. Zabusky, Phys. Rev. Lett. 27, 397 (1971).
[4]G. Joyce and D. Montgomery, J. Plasma Phys. 10, 107 (1973).
[5]J. P. Christiansen and J. B. Taylor, Plasma Phys. 15, 585 (1973).
[6]See, for example, L. D. Landau and I. M. Lifshitz, *Statistical Physics* (Addison-Wesley, Reading, Mass., 1958), p. 35.
[7]S. F. Edwards and J. B. Taylor, Proc. Roy. Soc., Ser. A 336, 257 (1974).
[8]D. Montgomery and G. Joyce, to be published.
[9]See, for example, N. Davidson, *Statistical Mechanics* (McGraw-Hill, New York, 1966), Chap. 21.
[10]G. A. Benford and D. L. Book, in *Advances in Plasma Physics*, edited by A. Simon and W. B. Thompson

(Wiley, New York, 1971), Vol. 4, p. 125.
[11]R. E. Lee and M. Lampe, Phys. Rev. Lett. 31, 1390 (1973).
[12]S. Fisher, Phys. Fluids 14, 962 (1971).
[13]B. Marder and H. Weitzner, Plasma Phys. 12, 435 (1970).
[14]L. Baker, private communication.
[15]B. E. McDonald, J. Comput. Phys. 16, 360 (1974).
[16]S. Fisher and D. L. Book, Bull. Amer. Phys. Soc. 19, 585 (1974).
[17]J. Norbury, private communication.
[18]C. Kittel, *Elementary Statistical Physics* (Wiley, New York, 1958), p. 115.
[19]R. H. Kraichnan, Phys. Fluids 10, 117 (1967).
[20]G. A. Williams and R. E. Packard, Phys. Rev. Lett. 33, 280 (1974).

Spin Diffusion and Spin Echoes in Superfluid ^{3}He†

Roland Combescot*
Laboratory of Atomic and Solid State Physics, Cornell University, Ithaca, New York 14853
(Received 14 November 1974)

The spin-diffusion coefficient for spin-echo experiments is calculated in the A phase and in the B phase of superfluid ^{3}He, using a relaxation-time approximation. Spin-wave attenuation is discussed for long wavelengths. It is pointed out that Leggett's result for the NMR lineshift is true over the complete range of frequency.

Spin waves in superfluid ^{3}He have recently been raising a growing theoretical interest.[1-5] However, the direct experimental detection of propagating spin waves does not seem to be very easy, at least in the A phase. The reason is that the spin-wave frequency has a lower bound which is the NMR longitudinal frequency $\omega_0(T)$. From the spin-wave velocity, it is found that the characteristic length in experiments is of order of 0.1 mm. This makes an experiment difficult although not impossible.

A less direct way of showing evidence for spin waves is to study spin diffusion, using the well-established spin-echo technique. This has been used successfully in normal ^{3}He: For still unclear reasons, spin-wave propagation (in a magnetic field) has not been detected directly, but the very good agreement between theory[6,7] and experiment[8] in spin-echo experiments leaves little doubt as to the actual existence of spin waves. Extending this idea to superfluid ^{3}He, I calculate in this paper the spin diffusion coefficient in a magnetic field in the superfluid phases by using a relaxation time approximation. I make the usual assumption that the A phase is the axial state [Anderson-Brinkman-Morel (ABM) state] and the B phase the isotropic state [Balian-Werthamer (BW) state], which seems to be more and more supported by experiments. This calculation is done in the regime of small departure from equilibrium. For spin-echo experiments, this means that the present results are only relevant to small tipping angles. Since the calculation of the spin-diffusion coefficient is merely an expansion to second order of the spin-wave dispersion relation for long wavelengths, my results provide, at the same time, the spin-wave attenuation at long wavelengths in a magnetic field. Finally, it is pointed out that Leggett's result for the NMR lineshift[9] is true beyond the hydrodynamic limit $\omega_L \tau_D \ll 1$ and extends to the collisionless limit if terms of order $[\omega_0(T)/\omega_L]^4$ are neglected (ω_L is the Larmor frequency).

The formalism that is used has been introduced already in preceding publications.[2,3,10] It is based on the kinetic-equation method and works only in the regime $\omega, qv_F \ll \Delta$, where Δ is the order parameter. In order to save space, I will not rewrite all the basic equations which are displayed in Ref. 3. However, I want to take into account collision terms in the kinetic equation. For this purpose, I will approximate the collision terms in the same way as in Ref. 10 and write the kinetic equation as

$$\omega \delta\vec{\nu}_k - \delta\vec{\nu}_k q_i \partial E_k/\partial k_i - i\delta\vec{E}^0 \times \delta\vec{\nu}_k = -i\delta\vec{\nu}_k/\tau_D(T) \quad (1)$$

with the same notations as in Ref. 3 and

$$\delta\vec{E}^0 = -(\xi_k/E_k)\vec{\omega}_L' - (1-\xi_k/E_k)\vec{d}_k(\vec{d}_k^* \vec{\omega}_L')/|\Delta_k|^2, \quad (2)$$